Emergence and clonal expansion of *Vibrio aestuarianus* lineages pathogenic for oysters in Europe.

Aurélie Mesnil[1,2], Maude Jacquot[1], Céline Garcia[1], Delphine Tourbiez[1], Lydie Canier[1], Audrey Bidois[2], Lionel Dégremont[1], Deborah Cheslett[3], Michelle Geary[3], Alessia Vetri[4], Ana Roque[5], Dolors Furones[5], Alison Garden[6], Petya Orozova[7], Isabelle Arzul[1], Mathieu Sicard[8], Guillaume Charrière[2], Delphine Destoumieux-Garzón[2], Marie-Agnès Travers[2*]

1 ASIM, Ifremer, Station de La Tremblade, avenue de Mus du Loup, 17390 La Tremblade, France

2 IHPE, Université de Montpellier, CNRS, IFREMER, Univ Perpignan Via Domitia, Montpellier, France

3 Marine Institute MI, Rinville, Oranmore, Co. Galway, H91 R673, Ireland

4 Istituto Zooprofilattico Sperimentale delle Venezie (IZSVe), Viale dell'Università 10, 35020 Legnaro (PD), Italy

5 IRTA La Ràpita. Aquaculture Program. 43540 – San Carles de la Ràpita, Spain.

6 Marine Laboratory, Marine Scotland Science, Aberdeen, UK.

7 National Diagnostic and Research Veterinary Medical Institute, Sofia, Bulgaria.

8 ISEM, Université de Montpellier, CNRS, IRD, Montpellier, France.

* Corresponding author: marie.agnes.travers@ifremer.fr

Competing interests: The authors declare no conflict of interest.

Abstract

Crassostrea gigas oysters represent a significant global food source, with 4.7 million tons harvested per year. In 2001, the bacterium *V. aesturianus francensis* emerged as a pathogen that causes adult oyster mortality in France and Ireland. Its impact on oyster aquaculture has increased in Europe since its reemergence in 2012. To better understand the evolutionary mechanisms leading to the emergence and persistence over time of this pathogen, we conducted a survey of mollusk diseases through national reference laboratories (NRLs) across Europe. We analyzed 54 new genomes of *V. aestuarianus* (*Va*) isolated from multiple environmental compartments since 2001, in areas with and without bivalve mortalities. We used a combination of comparative genomics and population genetics approaches to show that *Va francensis* lineages have undergone clonal expansion in Europe, likely after a recent selective bottleneck. Low mutation and recombination rates may have selected particular virulent genotypes. Furthermore, we identified a specific *cus-cop*-containing island conferring copper resistance to *Va francensis* whose acquisition may have favored the emergence of pathogenic lineages adapted to oysters.

Introduction

Marine populations are under increasing threat of emerging infectious disease (EID) (1), contributing to mass mortality events impacting corals, sea-stars, mollusks and fish (2-4). Aquaculture is practiced in an open and highly connected environment and thus particularly threatened by pathogen propagation (5). Moreover, aquacultural practices frequently result in high population densities and many animal transfers, increasing the risk of pathogen introduction and dispersal (6).

Oysters (*Crassostrea gigas*) are frequently impacted by bacterial pathogens of the genus *Vibrio* (7-9). Vibrios are ubiquitously distributed in the oceans and show a wide range of niche specialization, ranging from free-living forms to those attachment to biotic and abiotic surfaces,

from symbionts to pathogens, and from estuarine inhabitants to deep-sea piezophiles living under high pressure (10). Among them, *Vibrio aestuarianus* subsp. *francensis (Va francensis)* has caused recurrent mortality of adult oysters since 2001 (11). Having previously been restricted to France, this disease has now spread across European countries (France, Italy, Ireland, and Spain) (12, 13). This spread of *Va francensis* has resulted in mortality rates of approximately 25% and is a major economic concern as it impacts market-size oysters (14). Previous field studies found that pathogenic strains of *Va francensis* can colonize sentinel oysters, but are rare in samples from the local environment, *i.e.* sediment and water column. These data suggest that oysters are the preferred habitat of this pathogen (15). Moreover, it has been proposed that *Va francensis* can persist in oyster tissues during winter (15). These observations suggest *Va francensis* has adapted to oysters and raise questions about how this host specialization has occurred.

The emergence of pathogenic bacterial lineages can follow the acquisition of new traits which increase the ability to colonize a host (16). Trait acquisition can be achieved by mutation (17), but it occurs more frequently through horizontal transfer (through transformation, conjugation or transduction) of one or more genes favoring rapid adaptation to new niches and hosts (18). After emergence, the dynamics of pathogenic lineages are dictated by the relative importance of evolutionary forces: mutation, selection, genetic drift and recombination. Populations whose evolution is not or little influenced by recombination evolve clonally (19). One of the factors limiting the rates of horizontal transfer and recombination in a population is ecological isolation (20, 21) which limits opportunity to exchange genetic material with other populations.

Previous studies on *V. aestuarianus* diversity were based on a limited number of genomes, not reflecting overall diversity across diverse isolation contexts (22). This lack of genomic data hinders a complete understanding of the mechanisms governing the emergence and evolutionary dynamics of pathogenic lineages in *Va francensis.*

77 In the present study, we analyzed 54 genomes of isolates collected since 2001 across Europe.
78 We combined phylogenetic and population genetic approaches to decipher evolutionary
79 processes associated with the origin of the emergence of this oyster pathogen. Our study
80 shows that *Va francensis* strains exhibit numerous features commonly reported in specialized
81 pathogens. In particular, our data suggest the acquisition of genes involved in copper
82 resistance is one mechanism promoting *V. aestuarianus* adaptation to oysters.

83 Results

84 European spread of *V. aestuarianus* oyster pathogens

85 To assess the geographic distribution of pathogenic *V. aestuarianus* in Europe, a
86 questionnaire was sent in 2021 to all European laboratories in charge of the diagnosis and
87 surveillance of mollusk diseases (supplementary material). Eight out of the 12 respondent
88 laboratories reported that *V. aestuarianus* was detected during adult oyster mortality events.
89 The earliest detections were reported by France and Ireland in 2001, and the most recent
90 detection was reported by Denmark in 2021 (case used DNA detection only) (fig. 1, A). The
91 number of countries reporting detection has increased since 2011, with 8 European countries
92 currently reporting *V. aestuarianus*. Importantly the date of first detection may be under-
93 estimated, since surveillance and testing for the pathogen has varied between countries and
94 was only implemented in the majority of the laboratories following the development of a
95 diagnostic tool in 2009 (23).

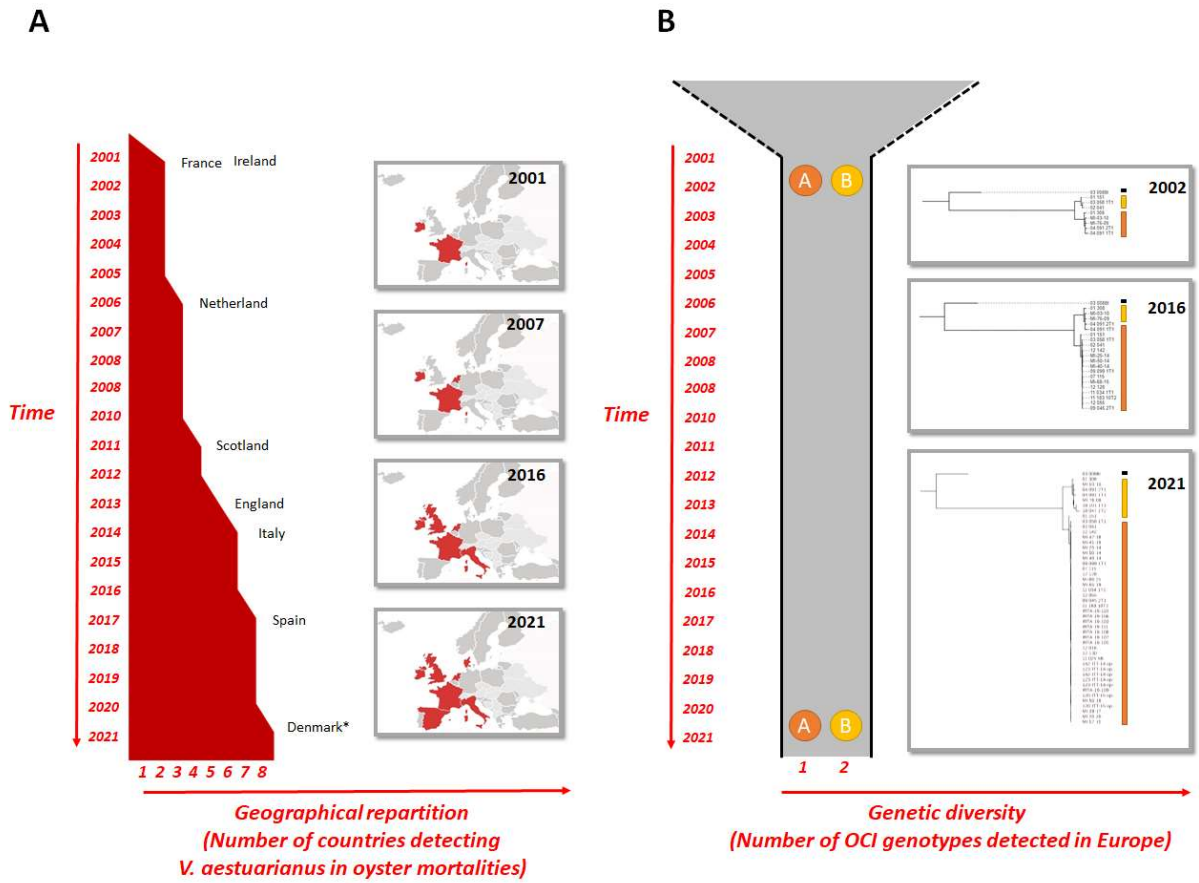

*Figure 1 : Figure 1: European expansion of V. aestuarianus francensis. While the geographic distribution of V. aestuarianus strains involved in C. gigas mortalities expands, genetic diversity remains stable over time. A) The number of countries reporting the detection of V. aestuarianus was assessed through a questionnaire sent to European national reference laboratories (NRLs). *Note: Denmark case report corresponds to a suspected case without bacterial isolation. B) The two lineage expansions: 2 genotypes were determined based on a maximum likelihood phylogenetic tree from complete genome alignments (GTR substitution model).*

V. aestuarianus diversity is structured according to environmental origin and isolation context.

In order to assess the overall population structure of *V. aestuarianus* in Europe, we studied genetic diversity at the whole genome level using *V. aestuarianus* isolates from a broad variety of origins. 54 strains were sequenced and genomes were *de novo* assembled. We obtained 15 4.5-Mb complete genomes (with 2 to 4 contigs) and 39 draft genomes (with up to 150 contigs) (table S1). Whole genomes were aligned, and relationships between isolates were studied by building a maximum likelihood phylogeny (fig. 2). Overall, genomes were close to

each other in the tree and showed highly similar nucleotide compositions, showing average nucleotide identities (ANIs) higher than 97.1% for all pairwise comparisons (table S2). The tree showed a tightly clustered clade of oyster clinical isolates (*i. e.*, isolates from moribund oysters) (n = 25) inside genetically diverse *V. aestuarianus* strains isolated outside of oyster mortalities (n = 29), encompassing non-clinical isolates (i.e. strains isolated from sites without mortalities) and strains isolated during cockles mortalities. All oyster clinical isolates are encompassed in *Va francensis* subspecies (24) and all *Va francensis* isolates were found in oysters, and showed higher virulence levels when assayed through injection into oyster muscle (p-value< 0.001). The reconstructed tree also confirmed that this subspecies is composed of two lineages named A (n = 17) and B (n = 8) (22).

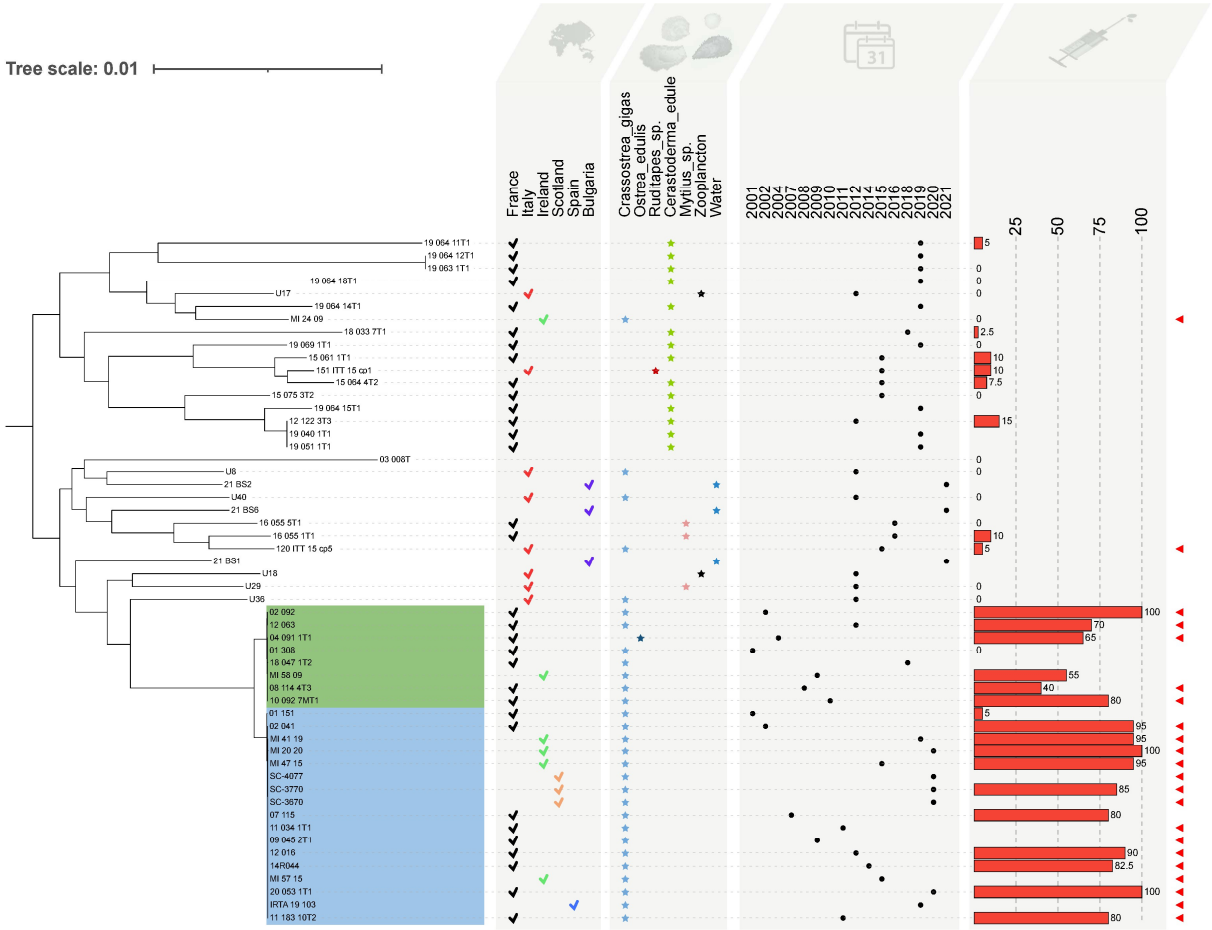

Figure 2 : V. aestuarianus diversity is structured according to host species and isolation context. Phylogenetic tree of V. aestuarianus species calculated with RAxML using a GTR substitution model and rooted with the midpoint rooting option from whole-genome alignments. Several layers of annotations are added: country (check mark), matrix of isolation (star), year of isolation (point), virulence

testing in the laboratory by injection into oysters (107 UFC/animal, duplicates of 10 animals) indicated with a bar plot on the right side representing mortality percentages, and context (strains isolated during oyster mortality events are indicated with a red arrow on the right). Va francensis lineages A and B are highlighted in blue and green, respectively. Their virulence is significantly higher compared to non clinical isolates (i. e. strains isolated on sites without mortalities) by Wilcoxon-Mann-Whitney test (p-value < 0.001). The absence of virulence data means the absence of a test for this strain.

116 Analysis of molecular variance (AMOVA) performed on the sequence dataset revealed that
117 the isolation context ("oyster mortality" or not) and environmental origin (five host species,
118 zooplankton and water) explained most significantly ($p < 0.005$) genetic variation (table 1).
119 AMOVA also indicated the absence of spatial and temporal delineation of the oyster pathogen
120 lineages. Altogether, our data reveal *V. aestuarianus* lineages linked European expansion of
121 this oyster pathogen.

Table 1 : Analysis of molecular variance supporting genetic partitioning according to environmental origin and isolation context

Factor	Variability (%)	p-value
Environmental origin	**17.8**	**0.002**
Isolation context	**16.0**	**0.001**
Country of isolation	7.1	0.074
Year of isolation	3.4	0.25

122

123 ## Temporal emergence of oyster pathogen lineages

124 Next, we used a Bayesian approach to date the emergence and reconstruct the temporal
125 evolution of oyster pathogens lineages. As a critical prerequisite, we checked whether the *Va*
126 *francensis* subspecies is a measurably evolving population. A temporal signal was observed
127 with a correlation between genetic distances from a reconstructed common ancestor and
128 strains sampling time, yielding a R^2 of 0.4236 (fig. S1A). The best-fitting evolutionary model
129 for the *Va francensis* population was obtained under a GMRF Bayesian skyline population
130 model with a relaxed clock, leading to a rate of 7.27×10^{-7} substitutions per position per year,
131 or 3.2 mutations per genome per year. The mean time of emergence of the most recent
132 common ancestor (TMRCA) of the lineage A was estimated to be 1956 (95% highest posterior
133 density (HPD): 1919–1972). At this time, a divergence occurred between strain 01-151, which
134 is non-virulent toward oysters, and other lineage A strains that are mostly pathogenic. The

135 TMRCA of lineage B maps to the late 1970s, albeit with uncertainty (95% HPD: 1898–1993).
136 According to the coalescence-based reconstruction of demographic variation, the *Va*
137 *francensis* population has slowly decline since its emergence, with accelerated decline since
138 2000 (fig S1B).

139 ## Genome stability in *V. aestuarianus francensis* lineages

140 Recombination can drive genetic diversity and evolutionary dynamics in bacterial populations.
141 We therefore quantified homologous recombination events using *V. aestuarianus* genome
142 alignments.

143 **Recombination has little impact on oyster pathogen evolution.** We found that
144 recombination (r) has a lower impact on the core genome substitution rate in *Va francensis*
145 lineages than the impact of mutation (m), with mean r/m = 0.36+/- 0.22 and 0.28+/- 0.09 in
146 lineages A and B respectively. The ratios of these lineages are significantly (student test p-
147 value < 0.005) smaller than in non-clinical *V. aestuarianus* isolates (i.e. strains isolated from
148 sites without mortalities) (r/m = 0.91 +/- 0.45). 7.8 and 3.3 recombination events were identified
149 on average for these lineages. Recombination in genomes can generate phylogenetic
150 inconsistencies between taxa that can emerge in phylogenetic networks as the presence of
151 alternative pathways (25). The network that we constructed from the whole-genome alignment
152 (fig. S2) confirmed that recombination does not affect *Va francensis* isolate relationships, with
153 few ambiguities among these taxa. One known consequence of the absence of recombination
154 impact is strong linkage between loci in non-recombinant genomes (26). In *Va francensis*
155 lineage A and, to a lesser extent, in lineage B, strong linkage between single nucleotide
156 polymorphisms (*SNPs*) was observed (fig. S3). In contrast, the recombination impact detected
157 in all other genomes was confirmed with phylogenetic networks, which showed ambiguities
158 between taxa (fig. S2) and low linkage between loci in these genomes (fig. S3). However,
159 recombination might have supported the emergence of the *Va francensis* group: 488
160 recombination events were detected at the node corresponding to the hypothetical common
161 ancestor of all pathogenic oyster isolates (fig. S4).

162

163 **Core genome stability was observed in *Va francensis* lineages.** Mutations also generated
164 little genetic diversity among *Va francensis*. Indeed, apart from the recombinant segments,
165 among the 19 775 variant genomic positions in the full dataset, 666 and 83 positions vary
166 among *Va francensis* A and B lineages. Finally, low impact of recombination and mutation on
167 *Va francensis* lineages results in core genome stability. We used Tajima's D to compare ob-
168 served genetic diversity in *V. aestuarianus* to that expected under neutral evolution and con-
169 stant population size. Deviation from neutrality was larger among the *Va francensis* lineages
170 A (Tajima's D = -2.3) and B (-2.5) than in the full dataset (-0.7), with less polymorphism than
171 expected under neutral evolution (fig. 3 A). To determine whether the low genetic diversity was
172 due to demographic effects (affecting whole genomes) or to selection effects (affecting partic-
173 ular genes), we adopted a gene-based approach to investigate selection pressures at the gene
174 level. While most of the 1,974 core genes were under neutral evolution outside of the *Va fran-*
175 *censis* subspecies, the vast majority were monomorphic within lineages A and B (fig. 3 B),
176 which is consistent with the purging of genetic diversity through bottlenecks during transmis-
177 sion dynamics.

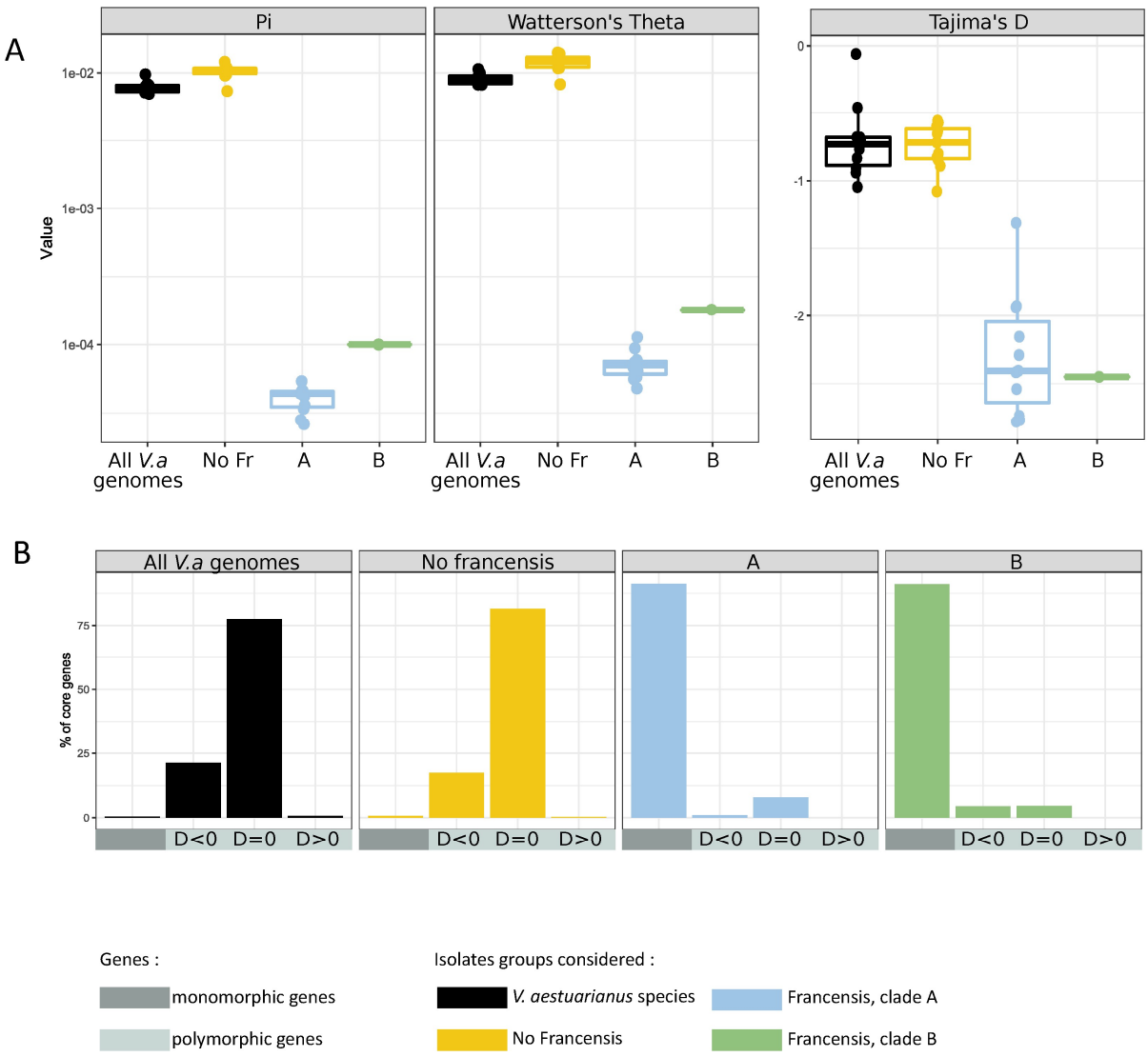

178

Figure 3 : Support for a recent bottleneck that purged genetic diversity in V. aestuarianus francensis lineages. Genetic statistics in V. aestuarianus species (black), other than Va francensis (yellow), Va francensis, lineage A (blue) and lineage B (green). A) Whole genome scale. Even through the expected genetic diversity under neutral evolution and a stable population size in Va francensis is low (Watterson's theta), the observed diversity (Pi) is still lower, as shown by the Tajima's D value below -2. Pi: observed genetic diversity; Theta_w: Watterson estimate of expected genetic diversity; Tajima_D: Tajima's D test statistic. The Y axis in the Pi and Watterson's theta plots is log10 scaled. B) Gene scale. Core genes show different selection patterns among groups of strains and among core genes within groups. While most core genes are under neutral evolution in isolates other than Va francensis, most genes are monomorphic in Va francensis lineage A and B. D>0 and D<0: significantly negative or positive Tajima's D value ($p < 0.05$) and D=0 ($p > 0.05$). A negative Tajima's D is indicative of purifying selection or recent population expansion, while a positive Tajima's D is indicative of diversifying selection or population contraction. A zero value is indicative of neutral evolution.

179 ***Va francensis* subspecies were found to have a closed pangenome**, with genes largely

180 shared among all isolates and almost no strain-specific genes, as determined by dataset

181 pangenome analysis (fig S5). In contrast, other *V. aestuarianus* isolates exhibited many strain-
182 specific genes. Altogether, our data support the clonal evolution of the two *Va francensis*
183 lineages.

184 **Positive selection signatures of oyster pathogen lineages**

185 We used *pcadapt,* which detects structure and clustering of individuals in a population, to
186 detect potential signatures of positive selection affecting oyster pathogen lineages. 2,925
187 SNPs were selected with an adjusted p-value <0.001. Based on principal component analysis,
188 principal component 1 (PC1) segregated the *Va francensis* lineages from the rest of *V.*
189 *aestuarianus* strain collection (fig. S6). 46 outlier SNPs were associated with PC1 including 17
190 non-synonymous and one stop-gained SNP potentially involved in diversifying selection.
191 These genes are listed in table S3 and notably include genes encoding flagellar proteins
192 (*pomA*) or related to chemiotaxis.

193 **Oyster-pathogenic *V. aestuarianus* have genomic features of specialist**
194 **pathogens**

195 According to low rates of homologous recombination and the closed pangenome, the two *Va*
196 *francensis* lineages can be considered as clonally evolving lineages. Furthermore, clonal
197 evolution, as well as the small number of known habitats (15), suggest that these lineages are
198 oyster specialists. Pathogen populations have often undergone a change of niche (passage
199 from a free-living lifestyle to an obligatory parasitic one), ultimately resulting in ecological
200 isolation and thus inhibition of DNA transfer with the parental population, or even with the
201 broader bacterial community (27, 28).
202 We further tested the hypothesis of specialization by analyzing genomic features known to be
203 enriched during transition to specialist lifestyle : insertion sequences (ISs) and pseudogene
204 (29). We found a higher number of ISs in the genomes of pathogenic oyster lineages A and B
205 than in strains isolated from contexts without bivalve mortality (p-value = 0.01 and 0.02,
206 respectively). Interestingly, in groups containing strains isolated during cockle mortality events,

207 ISs were more abundant than in pathogenic oyster genomes (p-value = 0.02 and 0.03,
208 respectively) (fig. 4). IS families were conserved between oyster pathogen genomes, with most
209 ISs belonging to the IS66, IS902 and ISAS1 families (table S4 and fig S7). IS conservation in
210 theses clades suggests that IS enrichment and expansion in genomes stopped after pathogen
211 emergence. The dynamics of the ISs appeared to be different in the cockle isolates. Indeed,
212 the number and families of ISs represented appeared to be poorly conserved. We suspect that
213 IS flux is active in cockle isolates, with ongoing horizontal exchange and intragenomic
214 expansion.
215 To check whether IS enrichment is involved in pseudogenization, we crossed IS and
216 pseudogene genomic coordinates and determined the number of ISs with pseudogenes
217 around them (from 2,000 bp before the IS start to 2,000 bp after the IS end) (table S5 and S6).
218 Regardless of the genome and chromosome considered, the vast majority (on average 86%)
219 of ISs had pseudogenes nearby. IS and pseudogene enrichment supports our hypothesis that
220 the *Va francensis* lineages are specialized toward oyster.

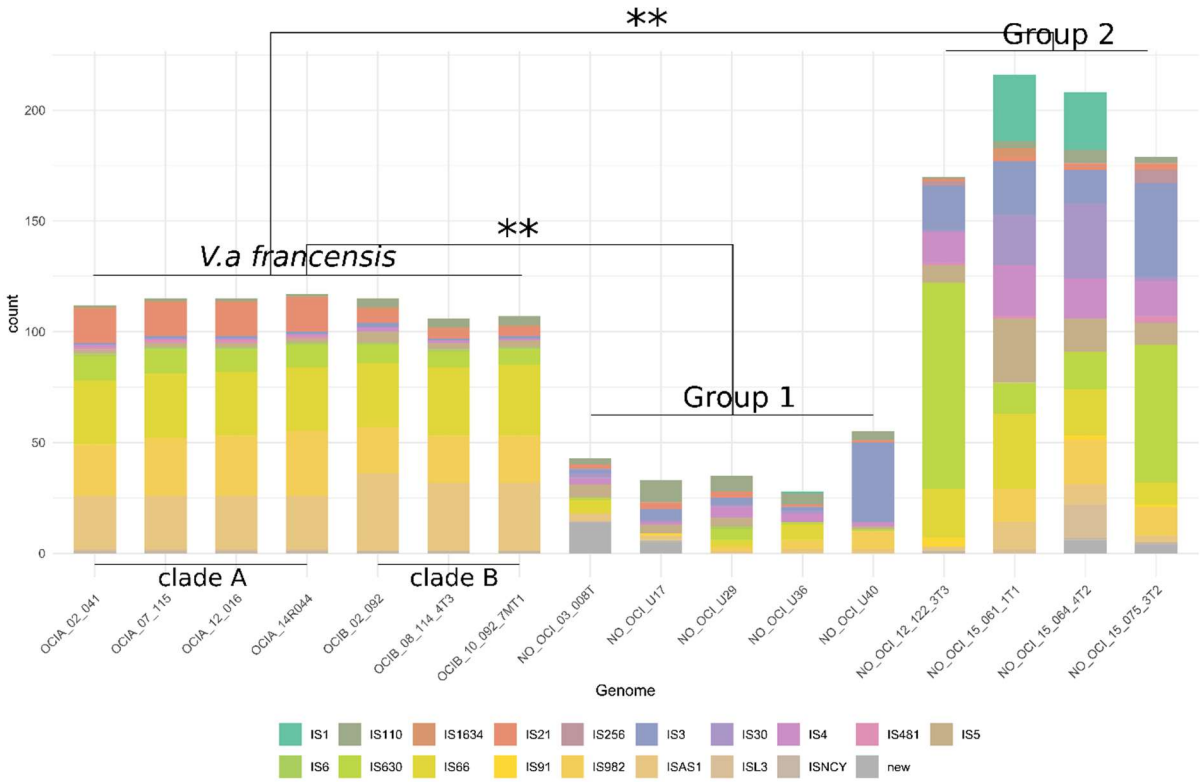

221

Figure 4 : Differential Insertion sequence (IS) enrichment is observed in Va francensis and cockle associated isolates genomes. Distribution of the number of IS elements (complete and partial) in 16

*complete genomes (chromosomes A and B). Colors represent IS families predicted by ISEScan. The genomes are those of 4 Va francensis lineage A strains, 3 Va francensis lineage B strains, 5 non clinical strains (isolated on sites without mortalities) (group 1), and 4 strains isolated during cockle mortality events (group 2). The conservation of IS number and families between genomes of Va francensis from lineage A or clade B indicates an ancestral origin of ISs. The genomes that contain the most ISs are those of strains isolated during cockle mortality events (group 2). The diversity of IS quantities and families represented suggests that IS enrichment is in progress. The number of ISs in groups was significantly different between Va francensis and other strains from group 1 and group 2 (**: Kruskal test p value < 0.05).*

222 **Copper resistance acquisition: One potential step in the emergence of oyster-**
223 **pathogenic clades**

224 Trait acquisition is often the first step preceding selective bottlenecks and clonal expansion of
225 host-adapted pathogens. To identify traits that may have preceded oyster pathogen
226 emergence, we studied the *V. aestuarianus* pangenome and detected 139 genes that were
227 shared exclusively by *Va francensis* genomes. Most of them (106) were annotated as
228 hypothetical proteins. The remaining 33 genes encode proteins with functions related to
229 copper export, cell-bacteria interaction (LPS/antigen O, cell wall or peptidoglycan), chemotaxis
230 and DNA repair. The sequences of these 139 genes were identical or well conserved between
231 strains (table S7).
232 Some oyster pathogen specific genes localize to a putative mobile genetic element (MGE), as
233 determined by crossing their coordinates with IS coordinates in an oyster pathogen genome
234 (02_041) (fig. 5 A). This putative MGE contains Cus operon genes (*cusABCF,S/R)* surrounded
235 by ISs from the IS66 family (length = 15 kb), as well as the copper export genes *copA* and
236 *copG* and the regulator *cueR*, located near tn7 transposon genes (tnA, B, C and E) (length =
237 10 kb), and is later referred to as a *cus-cop*-containing island.
238 The *Va francensis* ancestor could have acquired copper export genes by horizontal transfer.
239 Presence in an MGE could have facilitated integration of these genes into the bacterial
240 genome. To investigate the origin of *cus-cop*-containing islands, we used BLAST analyses of
241 each operon and of the entire region in 127 reference genomes of different *Vibrio* species
242 (table S8 and fig S8). The *cus-cop*-containing island presence is scattered along the *Vibrio*
243 phylogeny and is not specific to a monophyletic group. It appeared highly similar to some *V.*

244 *fluvialis* and *V. furnissii* genomic sequences with a nucleotide identity >95%. Moreover, this
245 region was close to plasmidic elements identified in *V. crassostreae* and *Vibrio* sp. dgh with a
246 nucleotide identity >89% (fig. 5B).
247 To test whether the genomic differences between the oyster pathogens and other strains could
248 lead to phenotypic differences, we tested copper resistance in 27 *V. aestuarianus* strains using
249 an agar diffusion assay. Supporting our hypothesis, all tested oyster pathogens (8 strains from
250 lineage A and 5 from lineage B) appeared significantly (p-value < 0.001) more resistant than
251 other strains to copper in radial diffusion assays (fig. 5C).

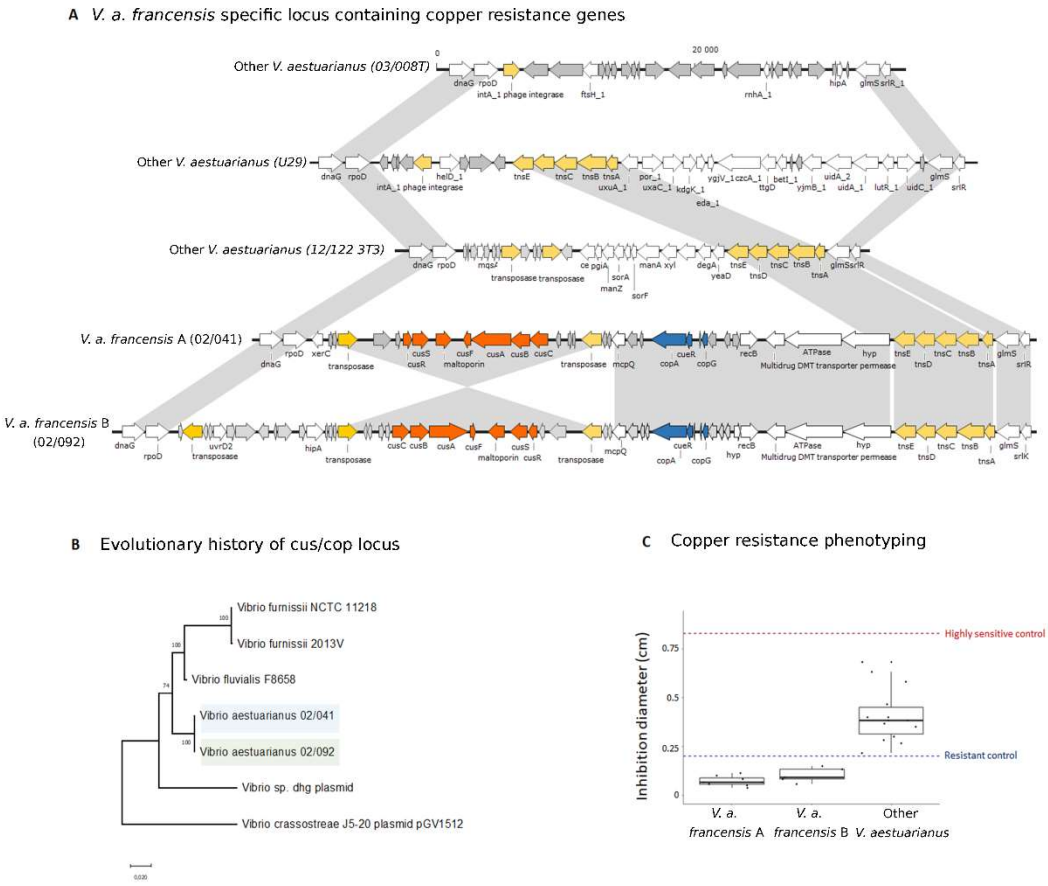

252

Figure 5 : A) Va francensis-specific locus containing copper resistance genes. Transposase and integrase are indicated in yellow, cus genes in orange, and cop genes in blue. B) Evolutionary history of the cus/cop locus. NJ, bootstrap test (500 replicates). The evolutionary distances were computed using the Kimura 2-parameter method and are shown as the number of base substitutions per site. This analysis involved 8 nucleotide sequences. All ambiguous positions were removed for each sequence pair (pairwise deletion option). There was a total of 29 555 positions in the final dataset. Evolutionary analyses were conducted in MEGA X [4]. C) Agar plate assay: bacterial growth inhibition diameter around a pellet impregnated with 50 mM CuSO4 solution. Va francensis linages A and B are significantly

more resistant to copper that other V. aestuarianus strains (Wilcoxon-Mann-Whitney test p value < 0.001).

253 ## Discussion

254 Here, we describe a genomic analysis of *V. aestuarianus* isolated from multiple European
255 countries, in different epidemic contexts and from multiple environments (five host species,
256 zooplankton and water) since 2001. We report the expansion and clonal evolution of two
257 oyster-pathogenic lineages from the *V. aestuarianus francensis* subspecies (11).

258 We estimate that 7.23 x 10^{-7} substitutions occur per site per year in *Va francensis*, similar to
259 the evolutionary rate inferred in *V. cholerae* during pandemic waves (30): this indicates that
260 pathogenic *Va francensis* lineages emerged during the 1990s, a decade when global oyster
261 production greatly increased according to Food and Agriculture Organisation. Indeed, oyster
262 production increased to over 140,000 tons per year in the 1990s (31). According to the
263 reconstructed demographic history, the effective population size of *Va francensis* is small and
264 showed a slowly decrease that accelerated in the 1990s. This sharper decreased may have
265 followed emergence of oyster-pathogenic lineages, indicating a possible bottleneck that
266 resulted in selection of oyster-adapted strains. This bottleneck may have purged
267 polymorphisms from this ancestral population, explaining the observed monomorphism in *Va*
268 *francensis* core genes. Indeed, some pathogenic monomorphic lineages may endure
269 population bottlenecks, supporting acquisition of new functions and colonization of new hosts
270 (32).

271 Several genomic modifications may help pathogenic oyster lineages adapt to their host,
272 including core genome substitutions and gene acquisition. We found non-synonymous
273 substitutions that were fixed in pathogenic oyster lineages. These occurred in genes involved
274 in host interaction or virulence, such as the *pomA* gene which encodes a flagellum motor
275 protein and the gene *luxP* linked to quorum-sensing. The functional consequences of these
276 substitutions remain to be explored.

277 Acquisition of copper resistance traits may also have contributed to the emergence of the
278 oyster-pathogenic lineages. Our data indicate that the *Va francensis* ancestor acquired a
279 genomic island carrying copper detoxification genes. Indeed, copper is a heavy metal found
280 at high levels in coastal waters because of agricultural and industrial activities (33-35). Copper
281 can accumulate in oyster tissues (up to 18,000 µg/g in China (36)), particularly at infection
282 sites (37) where it supports antimicrobial defense as copper can kill invading microorganisms
283 (37-39). Bacteria have, in turn, developed copper detoxification mechanisms which utilize the
284 *cop* and *cus* genes (40). *Cop* genes support initial Cu^+ translocation from the cytoplasm to the
285 periplasm. *Cus* genes encode a CusABC system that exports periplasmic copper into the
286 extracellular medium (41). Importantly, *copA* is essential for copper resistance, oyster
287 colonization and virulence in *V. tasmaniensis* LGP32, an oyster-pathogenic strain associated
288 with the Pacific Oyster Mortality Syndrome (42). Similarly, *copA* deletion in *V. crassostreae*
289 also attenuates virulence in oysters (7). Our data further support copper resistance as a shared
290 trait that allows pathogens to adapt to oysters as a host.

291 Our results suggest clonal evolution in *Va francensis* lineages. Recombination has a low
292 impact on genetic diversity. The r/m ratio, ~0.3 in both lineages, is similar to clonally evolving
293 pathogenic bacteria like the *V. cholerae* 7 pandemic lineage (r/m = 0.1 ; (43)), *M. tuberculosis*
294 complex (between 0,426 and 0,565, (44)) and lineage 1 of *Salmonella enterica* (r/m = 0.2 ;
295 (45)). We also found that *Va francensis* has a closed pangenome. This led us to formulate the
296 hypothesis of an ecological isolation of these lineages, a hallmark of specialized pathogens
297 that do not exchange genes with other bacterial populations. This hypothesis is also supported
298 by enrichment of insertion sequences and pseudogenization in both oyster-pathogenic
299 lineages. During specialization, pathogens transition from a free-living lifestyle to a permanent
300 association with a host. Through host association, pathogens can acquire compounds of
301 intermediate metabolism that allow genes associated with related biosynthetic pathways to
302 become facultative or redundant (25). Studies on pathogen specialization have largely focused
303 on highly specialized intracellular bacteria, which can undergo an extreme genome

304 rationalization process (26). This process implies pseudogenization of non-essential genes
305 that accumulate mutations or ISs and can ultimately result in gene loss (29, 46, 47). However,
306 genome size reduction was not observed, probably because *Va francensis* pathogenic
307 lineages are not obligate intracellular parasites. While oyster pathogens have a restricted
308 habitat, they can still replicate in the absence of their host, at least in rich medium. Moreover,
309 *Va francensis* can colonize diverse host tissues, including hemolymph, gills and digestive
310 connective tissues (15). As a consequence, *Va francensis* is adapted to diverse tissular micro-
311 environments, consistent with being less specialized than obligate intracellular bacteria.
312 Further studies of oyster pathogen microhabitats may help to elucidate their complete intra-
313 host life cycle, and the functions of specific genes linked to adaptation. Whether clades A and
314 B occupy similar niches in infected oysters and whether they have the potential to cooperate
315 remains unknown. Neither epidemiological parameter estimation (48) nor in-depth analysis of
316 their genomes identified lineage-specific functional traits.

317 Here we report the clonal expansion of *Va francensis* lineages across Europe. It has been
318 reported that another major pathogen, the herpes virus Ostreid OsHV-1, has also caused the
319 mortality of *C. gigas* (49) along the French coasts since the emergence of a new variant in
320 2008 (50). Double infections by OsHV-1 and *Va francensis* were reported in French oyster
321 farms in 2014 and 2015 (51, 52) and have also been observed in Ireland since 2008 (Cheslett,
322 pers comm). Although experimental infections combining the two pathogens at high doses in
323 spat and juvenile *C. gigas* have not demonstrated direct collaboration between them (53, 54),
324 at the population level the virus may still weaken animal defenses and thus amplify the impact
325 of *Va francensis*.

326 The global spread of pathogens is a recurrent problem in agriculture and aquaculture and is
327 often favored by anthropogenic introductions via infected hosts (55). The many transfers taking
328 place during the lifetime of an oyster probably explain most of the spread of pathogenic
329 lineages of *Va francensis* across Europe. Preventing the spread of pathogens during transfers
330 is particularly complicated in the case of *Va francensis* since the animals may be asymptomatic

331 (15). There is therefore an urgent need to develop sensitive detection assays to monitor the
332 spread of pathogens: the specific *Va francensis* genes revealed in this study, such as the
333 cusS/R genomic island, may provide new diagnostic tools, which may help to monitor and
334 prevent future mortality events.

335

336 Material & methods

337 Isolate selection

338 The study collection was designed to represent the temporal, geographic and clinical
339 heterogeneity of *V. aestuarianus* origins. However, ascertainment bias could occur due to
340 sampling strategy used. Indeed, strains were mainly isolated during bivalve mortalities. We
341 maximized recovery of the genetic diversity of oyster pathogenic *V. aestuarianus* by collecting
342 isolates from all European countries reporting mortalities related to *V. aestuarianus* or
343 presence of the bacteria. We also included strains isolated during field surveys of sites without
344 known mortality events. Strains were collected with the help of European NRLs responsible
345 for the diagnosis and surveillance of mollusk diseases: Ifremer (France), MI (Ireland), IZSVE
346 (Italy), IRTA (Spain), Marine Scotland Science (Scotland), and NRLFMC (Bulgaria). Sequence
347 comparisons of isolates from France, notably those isolated from moribund oysters, turned out
348 to be very similar. In order to equilibrate our sampling, we excluded 17 isolates identical with
349 included isolates. We selected approximately one strain per batch of moribund oysters (a batch
350 represents a sampling point) (table S9). The 54 isolates used in the study are summarized in
351 table S10.

352 Illumina, Ion torrent and PacBio whole-genome sequencing

353 Genome sequencing was performed between 2019 and 2021. Several sequencing
354 technologies were used depending on the objectives. We used a long-read sequencing

355 technology for some strains to improve assembly quality and study genomic features. DNA
356 was isolated from 35 strains using the NucleoSpin Tissue Kit (Macherey-Nagel) following the
357 manufacturer's guidelines. The concentration of each sample was adjusted to 0.2 ng/µl for
358 library preparation using the Illumina Nextera XT DNA Library Preparation Kit according to the
359 manufacturer's guidelines. For each library, paired-end reads of 150 bp were produced on the
360 Illumina NextSeq 550 platform (Bio Environnement, Perpignan, France). The quality of the
361 resultant fastq files was assessed using FastQC (56). Primers, Illumina adapter sequences,
362 low-quality bases at the 3′ end of reads with Phred-scaled quality scores less than 30 and
363 reads with a length <50 bp were removed using Trim Galore (57). Quality-controlled reads
364 were *de novo* assembled using the SPAdes genome assembler v3.13.1 (58) with the default
365 kmer size and a coverage cutoff value of 20 reads (59).
366 For 2 strains (04_091_1T1 and U8), enzymatic shearing was performed on 500ng of genomic
367 bacterial DNA using the NEBNext Fast DNA Library Prep kit (New Englands Biolabs) and
368 following the manufacturer's recommendations. Samples were barcoded with individual
369 IonCodes (Thermo). Purified libraries were then quantified by real-time PCR using the Ion
370 Universal Library Quantification Kit (Thermo) prior to be diluted and pooled at 25µM each. The
371 Ion Torrent S5 libraries were prepared using the "Ion 510™ & Ion 520™ & Ion 530™" for Ion
372 Chef Kit and sequenced on the Ion Torrent S5 using an Ion 530 semi-conductor sequencing
373 chip (Thermo).
374 DNA was isolated from other strains using a MagAttract HMW DNA Kit (Qiagen) following the
375 manufacturer's instructions. Library preparation and sequencing on a PacBio Sequel II
376 instrument were performed with the GENTYANE INRAe platform (Clermont-Ferrand, France).
377 *De novo* genome assemblies were obtained using FLYE v2.8.3 (60). One round of polishing
378 was performed using RACON v 1.4.3 (61).
379 The assembly was evaluated with QUAST, and genome completeness was checked using the
380 BUSCO v5.1.1 (62) and vibrionales_odb10 databases as lineage datasets, including 57
381 Vibrionales as detailed in table S11.
382 Assembly features and GenBank accession numbers are summarized in table S1.

383 ## Genome annotations

384 For each assembly, coding sequences (CDSs) were predicted using PROKKA v1.12 (63) with
385 default databases and –compliant and –rfam flags and annotation of rRNAs, tRNAs and other
386 ncRNAs enabled. Functional annotation of the detected CDSs was performed using EggNog-
387 Mapper v2.1.0 (64, 65). ISs were detected in the genomes using ISEScan v1.7 (66).
388 Pseudogene detection was performed with the GenBank files released from PROKKA with
389 PSEUDOFINDER v1.0 (67) , using the diamond flag and NCBI nonredundant database.
390 These later analyses were performed only on resolved genomes to avoid obtaining false
391 negatives in IS detection and false positives in pseudogene detection at the intercontig
392 locations.

393 ## Phylogeny and recombination analysis

394 Pairwise ANIs (%) were calculated using FastANI (68). Whole-genome alignments of the 54
395 isolate contigs were made using Progressive Mauve v13/02/2015 (69). Whole-genome
396 alignment was used to infer the maximum likelihood phylogeny using RAxML v8.2.12 with the
397 TVM model of nucleotide substitution (transversion model, AG=CT and unequal base
398 frequencies) and 100 bootstrap replicates, with strain 03_008T as the outgroup.
399 To identify polymorphic sites, the haploid variant calling pipeline snippy v4.6 (available at
400 https://github.com/tseemann/snippy) was used with default parameters.
401 To assess the influence of various structuring factors on the observed genetic diversity, we
402 performed AMOVA on the sequence dataset, with environmental origin, isolation context,
403 sampling year, and country as structuring factors, using the R package *pegas*.
404
405 Recombination was evaluated across this genome alignment using ClonalFrameML v1.12
406 (70). We used an extension that allows different recombination parameters to be inferred on
407 different branches of the clonal genealogy. Linear regression analysis of the root-to-tip
408 distances against sampling time was performed using TempEst v1.5.3 (71). The substitution

409 rate was estimated under different demographic and clock models, using Beast v1.10.4, taking
410 advantage of the sampling timeframe between 2001 and 2021. We tested both a strict and a
411 relaxed molecular clock. Constant-sized, exponential-sized and GMRF Bayesian skyride plot
412 models (72, 73) were used. For each model, two independent chains were conducted for 200
413 million generations and convergence was assessed by checking effective sample size values
414 for key parameters using Tracer v1.7.1 (74). For robust model selection, both path sampling
415 and stepping-stone sampling approaches were applied to each BEAST analysis to estimate
416 the marginal likelihood (75, 76). The best model selected by Bayes factor comparison was a
417 relaxed molecular clock with a GMRF Bayesian skyride demographic model. For this model,
418 triplicate runs were combined using LogCombiner v1.10.4, with removal of 10% burn-in.

419 **Selection analysis**

420 Tajima's D was calculated considering core genome alignment using MEGA 11 Tajima's test
421 on neutrality. Core genome alignment were previously partitioned according to lineages or
422 subspecies, resulting in *Va francensis* lineage A alignment (n = 17 sequences), *Va francensis*
423 lineage B alignment (n = 8 sequences) and no *Va francensis* alignment (n = 29 sequences).
424 Since sample size is known to influence population genetic parameter estimations (77), we
425 calculated Tajima's D on subsamples of eight sequences. For *Va francensis* lineage A and no
426 *Va francensis* isolates, Tajima's D was calculated on ten different alignments constructed with
427 eight sequences randomly subsampled. Then we calculated mean of the Tajima's D obtained
428 from the ten alignments. For the *Va francensis* lineage B alignment, the eight sequences
429 represented the entire sampled set. Tajima's D was also calculated for each core genes,
430 considering the same partitions, employing the R package *pegas*.
431
432 In order to detect SNPs that may explain *Va francensis* emergence, we performed a genome
433 scan analysis using *pcadapt* package v.4.3.3 for R (78) that detect structure and clustering of
434 individuals in a population. Number of principal components was set to six. We used
435 LD.clumping option, with window size of 5 kb. LD.clumping uses p-value to sort the SNPs by

436 importance (e.g. keeping the most significant ones). It takes the first one (e.g. most significant
437 SNP) and removes SNPs that are too correlated with this one in a window around it. We also
438 removed SNP with minor allele frequency under 0.05. After computing the test statistic, we
439 used Bonferroni adjustment to correct for multiple comparisons, and threshold of 0.001 was
440 applied to identify outliers SNPs.

441 **Bacterial virulence estimation by injection**

442 Bacteria were grown with constant agitation at 22°C for 24 h in Zobell medium. Cultures were
443 washed by centrifugation (10 min, 1500 g) and resuspended in artificial, sterile seawater to
444 obtain OD_{600nm} = 0.1. Fifty microliters of bacterial suspensions (10^7 cfu, checked by plating on
445 Zobell agar) were injected intramuscularly into anesthetized specific pathogen-free (SPF)
446 oysters produced and maintained in the IFREMER facility (79). After injection, the oysters were
447 transferred to aquaria (10 oysters per 2.5 L aquarium, duplicate aquaria per bacterial strain)
448 containing 2 L of aerated, UV-treated seawater at 22°C and kept under static conditions for 5
449 days.

450 **Copper resistance phenotyping**

451 Paper discs (6 mm) were loaded with $CuSO_4$ by soaking them overnight in 50 mM $CuSO_4$.
452 Cells from stationary phase cultures at DO = 1 were washed twice with SSW before being
453 spread onto agar plates containing 15 $g.L^{-1}$ bactopeptone and 0.5 M NaCl. Using sterile
454 tweezers, copper-impregnated disks were placed on the bacterial lawn before incubation at
455 20°C. After 5 days of incubation, the diameter of the inhibition zone around the disk was
456 measured.

457 **Statistic tests**

458 Basic statistical analysis of all of the data were performed using R v4.1.2. Data were checked
459 for normality and homogeneity of variance before analysis. Wilcoxon-Mann-Whitney was
460 performed to evaluate if recombination ratios, IS number in genomes, virulence toward oysters

461 and halo size (representing strains sensitivity to copper) differed among *Va francensis*
462 lineages and between *Va francensis* lineages and other strains.

Acknowledgments

We first thank the NRLs for mollusk diseases that contributed to the questionnaire survey (Bojan Adžić, Raquel Aranguren, Giuseppe Arcangeli, Deborah Cheslett, Marc Engelsma, Mark Fordyce, Ana Grade, Michael Gubbins, Lone Madsen, Petya Orozova, and Ewa Paździor). We thank Nicolas Bierne for helpful discussion and Viviane Boulo, Jean-Michel Escoubas, Nicole Faury and Gaelle Courtay for their valuable technical assistance. We also thank Bruno Petton and staff of IFREMER Bouin, who contributed to animal production and delivery. We thank the Bio-Environment platform (University of Perpignan Via Domitia) and Jean-François Allienne for support in library preparation and sequencing. We are grateful to the Ifremer Bioinformatics Core Facility (SeBiMER; https://ifremer-bioinformatics.github.io/) for providing technical assistance and scientific support in bioinformatics analysis. We also acknowledge the Pôle de Calcul et de Données Marines (https://wwz.ifremer.fr/en/Research-Technology/Research-Infrastructures/Digital-infrastructures/Computation-Centre) for providing DATARMOR computing and storage resources. This work was funded by Europe DG-Sante (through European Union Reference Laboratory for mollusk diseases funding) and French Ministry DPMA (MIRAGE project) and DGAl through NRL funding. Moreover, A.M., PhD, was supported by IFREMER and Région Nouvelle Aquitaine. This study is part of the « Laboratoire d'Excellence (LabEx) » TULIP (ANR-10-LABX-41) framework.

Bibliographic references

1. Le Roux F, Wegner KM, Baker-Austin C, Vezzulli L, Osorio CR, Amaro C, Ritchie JM, Defoirdt T, Destoumieux-Garzón D, Blokesch M. 2015. The emergence of Vibrio pathogens in Europe: ecology, evolution, and pathogenesis (Paris, 11–12th March 2015). Frontiers in microbiology 6:830.
2. Frans I, Michiels CW, Bossier P, Willems KA, Lievens B, Rediers H. 2011. *Vibrio anguillarum* as a fish pathogen: virulence factors, diagnosis and prevention. Journal of Fish Diseases 34:643-661.
3. Hewson I, Button JB, Gudenkauf BM, Miner B, Newton AL, Gaydos JK, Wynne J, Groves CL, Hendler G, Murray M, Fradkin S, Breitbart M, Fahsbender E, Lafferty KD, Kilpatrick AM, Miner CM, Raimondi P, Lahner L, Friedman CS, Daniels S, Haulena M, Marliave J, Burge CA, Eisenlord ME, Harvell CD. 2014. Densovirus associated with sea-star wasting disease and mass mortality. Proceedings of the National Academy of Sciences of the United States of America 111:17278-17283.
4. Lafferty KD, Kuris AM. 1993. Mass mortality of abalone Haliotis cracherodii on the California Channel Islands: tests of epidemiological hypotheses. Marine Ecology-Progress Series 96:239-239.
5. Lafferty KD, Harvell CD, Conrad JM, Friedman CS, Kent ML, Kuris AM, Powell EN, Rondeau D, Saksida SM. 2015. Infectious Diseases Affect Marine Fisheries and Aquaculture Economics. Annual Review of Marine Science 7:471-496.
6. Murray AG, Peeler EJ. 2005. A framework for understanding the potential for emerging diseases in aquaculture. Preventive Veterinary Medicine 67:223-235.
7. Bruto M, James A, Petton B, Labreuche Y, Chenivesse S, Alunno-Bruscia M, Polz MF, Le Roux F. 2017. *Vibrio crassostreae,* a benign oyster colonizer turned into a pathogen after plasmid acquisition. The ISME Journal 11:1043-1052.
8. Lemire A, Goudenège D, Versigny T, Petton B, Calteau A, Labreuche Y, Le Roux F. 2015. Populations, not clones, are the unit of vibrio pathogenesis in naturally infected oysters. The ISME Journal 9:1523-1531.
9. Petton B, Bruto M, James A, Labreuche Y, Alunno-Bruscia M, Le Roux F. 2015. *Crassostrea gigas* mortality in France: the usual suspect, a herpes virus, may not be the killer in this polymicrobial opportunistic disease. Frontiers in microbiology 6:686.
10. Reen FJ, Almagro-Moreno S, Ussery D, Boyd EF. 2006. The genomic code: inferring Vibrionaceae niche specialization. Nat Rev Microbiol 4:697-704.
11. Garnier M, Labreuche Y, Nicolas JL. 2008. Molecular and phenotypic characterization of *Vibrio aestuarianus* subsp. *francensis* subsp. nov., a pathogen of the oyster *Crassostrea gigas*. Syst Appl Microbiol 31:358-65.
12. Lasa A, di Cesare A, Tassistro G, Borello A, Gualdi S, Furones D, Carrasco N, Cheslett D, Brechon A, Paillard C, Bidault A, Pernet F, Canesi L, Edomi P, Pallavicini A, Pruzzo C, Vezzulli L. 2019. Dynamics of the Pacific oyster pathobiota during mortality episodes in Europe assessed by 16S rRNA gene profiling and a new target enrichment next-generation sequencing strategy. Environ Microbiol 21:4548-4562.
13. Mandas D, Salati F, Polinas M, Sanna MA, Zobba R, Burrai GP, Alberti A, Antuofermo E. 2020. Histopathological and Molecular Study of Pacific Oyster Tissues Provides Insights into *V. aestuarianus* Infection Related to Oyster Mortality. Pathogens 9.
14. Dégremont L, Azéma P, Maurouard E, Travers M-A. 2020. Enhancing resistance to *Vibrio aestuarianus* in *Crassostrea gigas* by selection. Aquaculture 526:735429.
15. Parizadeh L, Tourbiez D, Garcia C, Haffner P, Dégremont L, Le Roux F, Travers M-A. 2018. Ecologically realistic model of infection for exploring the host damage caused by *Vibrio aestuarianus*. Environmental Microbiology 20:4343-4355.
16. Engering A, Hogerwerf L, Slingenbergh J. 2013. Pathogen-host-environment interplay and disease emergence. Emerging microbes & infections 2:e5-e5.

534 17. Sheppard SK, Guttman DS, Fitzgerald JR. 2018. Population genomics of bacterial
535 host adaptation. Nature Reviews Genetics 19:549-565.
536 18. Martínez JL. 2013. Bacterial pathogens: from natural ecosystems to human hosts.
537 Environmental Microbiology 15:325-333.
538 19. Tibayrenc M, Ayala FJ. 2012. Reproductive clonality of pathogens: A perspective on
539 pathogenic viruses, bacteria, fungi, and parasitic protozoa. Proceedings of the
540 National Academy of Sciences 109:E3305-E3313.
541 20. Cohan FM. 2002. Sexual isolation and speciation in bacteria. Genetics of Mate
542 Choice: From Sexual Selection to Sexual Isolation:359-370.
543 21. Polz MF, Alm EJ, Hanage WP. 2013. Horizontal gene transfer and the evolution of
544 bacterial and archaeal population structure. Trends Genet 29:170-5.
545 22. Goudenège D, Travers MA, Lemire A, Petton B, Haffner P, Labreuche Y, Tourbiez D,
546 Mangenot S, Calteau A, Mazel D, Nicolas JL, Jacq A, Le roux F. 2015. A single
547 regulatory gene is sufficient to alter *Vibrio aestuarianus* pathogenicity in oysters.
548 Environ Microbiol 17:4189-99.
549 23. Saulnier D, De Decker S, Haffner P. 2009. Real-time PCR assay for rapid detection
550 and quantification of Vibrio aestuarianus in oyster and seawater: A useful tool for
551 epidemiologic studies. Journal of Microbiological Methods 77:191-197.
552 24. Garnier M, Labreuche Y, Garcia C, Robert M, Nicolas JL. 2007. Evidence for the
553 involvement of pathogenic bacteria in summer mortalities of the Pacific oyster
554 Crassostrea gigas. Microb Ecol 53:187-96.
555 25. Moran NA. 2002. Microbial minimalism: genome reduction in bacterial pathogens.
556 Cell 108:583-6.
557 26. Floriano AM, Castelli M, Krenek S, Berendonk TU, Bazzocchi C, Petroni G, Sassera
558 D. 2018. The Genome Sequence of "Candidatus *Fokinia solitaria*": Insights on
559 Reductive Evolution in Rickettsiales. Genome Biol Evol 10:1120-1126.
560 27. Hauck S, Maiden MCJ. 2018. Clonally Evolving Pathogenic Bacteria, p 307-325. *In*
561 Rampelotto PH (ed), Molecular Mechanisms of Microbial Evolution doi:10.1007/978-
562 3-319-69078-0_12. Springer International Publishing, Cham.
563 28. Bergstrom CT, McElhany P, Real LA. 1999. Transmission bottlenecks as
564 determinants of virulence in rapidly evolving pathogens. Proceedings of the National
565 Academy of Sciences 96:5095-5100.
566 29. Bäumler A, Fang FC. 2013. Host Specificity of Bacterial Pathogens. Cold Spring
567 Harbor Perspectives in Medicine 3.
568 30. Mutreja A, Kim DW, Thomson NR, Connor TR, Lee JH, Kariuki S, Croucher NJ, Choi
569 SY, Harris SR, Lebens M, Niyogi SK, Kim EJ, Ramamurthy T, Chun J, Wood JL,
570 Clemens JD, Czerkinsky C, Nair GB, Holmgren J, Parkhill J, Dougan G. 2011.
571 Evidence for several waves of global transmission in the seventh cholera pandemic.
572 Nature 477:462-5.
573 31. FranceAgriMer. 2021. https://www.franceagrimer.fr/. https://www.franceagrimer.fr/.
574 Accessed
575 32. Namouchi A, Didelot X, Schöck U, Gicquel B, Rocha EP. 2012. After the bottleneck:
576 Genome-wide diversification of the Mycobacterium tuberculosis complex by mutation,
577 recombination, and natural selection. Genome Res 22:721-34.
578 33. Claisse D, Alzieu C. 1993. Copper contamination as a result of antifouling paint
579 regulations? Marine Pollution Bulletin 26:395-397.
580 34. Hall LW, Anderson RD. 1999. A Deterministic Ecological Risk Assessment for
581 Copper in European Saltwater Environments. Marine Pollution Bulletin 38:207-218.
582 35. Rossi N, Jamet J-L. 2008. *In situ* heavy metals (copper, lead and cadmium) in
583 different plankton compartments and suspended particulate matter in two coupled
584 Mediterranean coastal ecosystems (Toulon Bay, France). Marine Pollution Bulletin
585 56:1862-1870.
586 36. Weng N, Wang W-X. 2014. Variations of trace metals in two estuarine environments
587 with contrasting pollution histories. Science of The Total Environment 485-486:604-
588 614.

589 37. Shi B, Wang T, Zeng Z, Zhou L, You W, Ke C. 2019. The role of copper and zinc
590 accumulation in defense against bacterial pathogen in the fujian oyster (*Crassostrea*
591 *angulata*). Fish Shellfish Immunol 92:72-82.
592 38. Destoumieux-Garzón D, Canesi L, Oyanedel D, Travers M-A, Charrière GM, Pruzzo
593 C, Vezzulli L. 2020. Vibrio–bivalve interactions in health and disease. Environmental
594 Microbiology 22:4323-4341.
595 39. Yeh S-T, Liu C-H, Chen J-C. 2004. Effect of copper sulfate on the immune response
596 and susceptibility to *Vibrio alginolyticus* in the white shrimp *Litopenaeus vannamei*.
597 Fish & Shellfish Immunology 17:437-446.
598 40. Bondarczuk K, Piotrowska-Seget Z. 2013. Molecular basis of active copper
599 resistance mechanisms in Gram-negative bacteria. Cell Biol Toxicol 29:397-405.
600 41. Argüello JM, Raimunda D, Padilla-Benavides T. 2013. Mechanisms of copper
601 homeostasis in bacteria. Front Cell Infect Microbiol 3:73.
602 42. Vanhove AS, Duperthuy M, Charriere GM, Le Roux F, Goudenege D, Gourbal B,
603 Kieffer-Jaquinod S, Coute Y, Wai SN, Destoumieux-Garzon D. 2015. Outer
604 membrane vesicles are vehicles for the delivery of Vibrio tasmaniensis virulence
605 factors to oyster immune cells. Environ Microbiol 17:1152-65.
606 43. Didelot X, Pang B, Zhou Z, McCann A, Ni P, Li D, Achtman M, Kan B. 2015. The
607 Role of China in the Global Spread of the Current Cholera Pandemic. PLOS Genetics
608 11:e1005072.
609 44. Namouchi A, Didelot X, Schöck U, Gicquel B, Rocha EPC. 2012. After the bottleneck:
610 Genome-wide diversification of the Mycobacterium tuberculosis complex by mutation,
611 recombination, and natural selection. Genome Research 22:721-734.
612 45. Didelot X, Bowden R, Street T, Golubchik T, Spencer C, McVean G, Sangal V, Anjum
613 MF, Achtman M, Falush D, Donnelly P. 2011. Recombination and Population
614 Structure in Salmonella enterica. PLOS Genetics 7:e1002191.
615 46. Siguier P, Gourbeyre E, Chandler M. 2014. Bacterial insertion sequences: their
616 genomic impact and diversity. FEMS Microbiology Reviews 38:865-891.
617 47. Touchon M, Rocha EPC. 2007. Causes of Insertion Sequences Abundance in
618 Prokaryotic Genomes. Molecular Biology and Evolution 24:969-981.
619 48. Travers MA, Tourbiez D, Parizadeh L, Haffner P, Kozic-Djellouli A, Aboubaker M,
620 Koken M, Degremont L, Lupo C. 2017. Several strains, one disease: experimental
621 investigation of *Vibrio aestuarianus* infection parameters in the Pacific oyster,
622 *Crassostrea gigas*. Vet Res 48:32.
623 49. Garcia C, Thébault A, Dégremont L, Arzul I, Miossec L, Robert M, Chollet B, François
624 C, Joly J-P, Ferrand S, Kerdudou N, Renault T. 2011. Ostreid herpesvirus 1 detection
625 and relationship with *Crassostrea gigas* spat mortality in France between 1998 and
626 2006. Veterinary Research 42:73.
627 50. Barbosa Solomieu V, Renault T, Travers MA. 2015. Mass mortality in bivalves and
628 the intricate case of the Pacific oyster, *Crassostrea gigas*. J Invertebr Pathol 131:2-
629 10.
630 51. Azéma P, Maurouard E, Lamy J-B, Dégremont L. 2017. The use of size and growing
631 height to improve *Crassostrea gigas* farming and breeding techniques against OsHV-
632 1. Aquaculture 471:121-129.
633 52. Azema P, Travers MA, De Lorgeril J, Tourbiez D, Degremont L. 2015. Can selection
634 for resistance to OsHV-1 infection modify susceptibility to *Vibrio aestuarianus*
635 infection in Crassostrea gigas? First insights from experimental challenges using
636 primary and successive exposures. Vet Res 46:139.
637 53. Azema P, Lamy JB, Boudry P, Renault T, Travers MA, Degremont L. 2017. Genetic
638 parameters of resistance to *Vibrio aestuarianus,* and OsHV-1 infections in the Pacific
639 oyster, *Crassostrea gigas*, at three different life stages. Genet Sel Evol 49:23.
640 54. Azéma P, Travers M-A, Benabdelmouna A, Dégremont L. 2016. Single or dual
641 experimental infections with *Vibrio aestuarianus* and OsHV-1 in diploid and triploid
642 *Crassostrea gigas* at the spat, juvenile and adult stages. Journal of Invertebrate
643 Pathology 139:92-101.

644 55. Anderson PK, Cunningham AA, Patel NG, Morales FJ, Epstein PR, Daszak P. 2004.
645 Emerging infectious diseases of plants: pathogen pollution, climate change and
646 agrotechnology drivers. Trends in Ecology & Evolution 19:535-544.
647 56. Wingett SW, Andrews S. 2018. FastQ Screen: A tool for multi-genome mapping and
648 quality control. F1000Res 7:1338.
649 57. Bush SJ. 2020. Read trimming has minimal effect on bacterial SNP-calling accuracy.
650 Microbial Genomics 6.
651 58. Bankevich A, Nurk S, Antipov D, Gurevich AA, Dvorkin M, Kulikov AS, Lesin VM,
652 Nikolenko SI, Pham S, Prjibelski AD, Pyshkin AV, Sirotkin AV, Vyahhi N, Tesler G,
653 Alekseyev MA, Pevzner PA. 2012. SPAdes: a new genome assembly algorithm and
654 its applications to single-cell sequencing. Journal of computational biology : a journal
655 of computational molecular cell biology 19:455-477.
656 59. Gurevich A, Saveliev V, Vyahhi N, Tesler G. 2013. QUAST: quality assessment tool
657 for genome assemblies. Bioinformatics 29:1072-5.
658 60. Kolmogorov M, Yuan J, Lin Y, Pevzner PA. 2019. Assembly of long, error-prone
659 reads using repeat graphs. Nature Biotechnology 37:540-546.
660 61. Vaser R, Sovic I, Nagarajan N, Sikic M. 2017. Fast and accurate de novo genome
661 assembly from long uncorrected reads. Genome Research
662 doi:10.1101/gr.214270.116.
663 62. Simão FA, Waterhouse RM, Ioannidis P, Kriventseva EV, Zdobnov EM. 2015.
664 BUSCO: assessing genome assembly and annotation completeness with single-copy
665 orthologs. Bioinformatics 31:3210-3212.
666 63. Seemann T. 2014. Prokka: rapid prokaryotic genome annotation. Bioinformatics
667 30:2068-2069.
668 64. Cantalapiedra CP, Hernández-Plaza A, Letunic I, Bork P, Huerta-Cepas J. 2021.
669 eggNOG-mapper v2: Functional Annotation, Orthology Assignments, and Domain
670 Prediction at the Metagenomic Scale. Molecular Biology and Evolution 38:5825-5829.
671 65. Huerta-Cepas J, Szklarczyk D, Heller D, Hernández-Plaza A, Forslund SK, Cook H,
672 Mende DR, Letunic I, Rattei T, Jensen Lars J, von Mering C, Bork P. 2018. eggNOG
673 5.0: a hierarchical, functionally and phylogenetically annotated orthology resource
674 based on 5090 organisms and 2502 viruses. Nucleic Acids Research 47:D309-D314.
675 66. Xie Z, Tang H. 2017. ISEScan: automated identification of insertion sequence
676 elements in prokaryotic genomes. Bioinformatics 33:3340-3347.
677 67. Syberg-Olsen MJ, Garber AI, Keeling PJ, McCutcheon JP, Husnik F. 2021.
678 Pseudofinder: detection of pseudogenes in prokaryotic genomes. bioRxiv
679 doi:10.1101/2021.10.07.463580:2021.10.07.463580.
680 68. Goris J, Konstantinidis KT, Klappenbach JA, Coenye T, Vandamme P, Tiedje JM.
681 2007. DNA-DNA hybridization values and their relationship to whole-genome
682 sequence similarities. Int J Syst Evol Microbiol 57:81-91.
683 69. Darling AE, Mau B, Perna NT. 2010. progressiveMauve: Multiple Genome Alignment
684 with Gene Gain, Loss and Rearrangement. PLOS ONE 5:e11147.
685 70. Didelot X, Wilson DJ. 2015. ClonalFrameML: Efficient Inference of Recombination in
686 Whole Bacterial Genomes. PLOS Computational Biology 11:e1004041.
687 71. Rambaut A, Lam TT, Max Carvalho L, Pybus OG. 2016. Exploring the temporal
688 structure of heterochronous sequences using TempEst (formerly Path-O-Gen). Virus
689 Evolution 2.
690 72. Minin VN, Bloomquist EW, Suchard MA. 2008. Smooth Skyride through a Rough
691 Skyline: Bayesian Coalescent-Based Inference of Population Dynamics. Molecular
692 Biology and Evolution 25:1459-1471.
693 73. Drummond AJ, Nicholls GK, Rodrigo AG, Solomon W. 2002. Estimating Mutation
694 Parameters, Population History and Genealogy Simultaneously From Temporally
695 Spaced Sequence Data. Genetics 161:1307-1320.
696 74. Rambaut A, Drummond AJ, Xie D, Baele G, Suchard MA. 2018. Posterior
697 Summarization in Bayesian Phylogenetics Using Tracer 1.7. Systematic Biology
698 67:901-904.

75. Baele G, Lemey P, Bedford T, Rambaut A, Suchard MA, Alekseyenko AV. 2012. Improving the Accuracy of Demographic and Molecular Clock Model Comparison While Accommodating Phylogenetic Uncertainty. Molecular Biology and Evolution 29:2157-2167.
76. Baele G, Li WLS, Drummond AJ, Suchard MA, Lemey P. 2012. Accurate Model Selection of Relaxed Molecular Clocks in Bayesian Phylogenetics. Molecular Biology and Evolution 30:239-243.
77. Subramanian S. 2016. The effects of sample size on population genomic analyses – implications for the tests of neutrality. BMC Genomics 17:123.
78. Paradis E. 2010. pegas: an R package for population genetics with an integrated–modular approach. Bioinformatics 26:419-420.
79. Petton B, Pernet F, Robert R, Boudry P. 2013. Temperature influence on pathogen transmission and subsequent mortalities in juvenile Pacific oysters *Crassostrea gigas*. Aquaculture Environment Interactions 3:257-273.